The Canadian Mineralogist
Vol. 45, pp. 857-864 (2007)
DOI: 10.2113/gscanmin.45.4.857

PITTONGITE, A NEW TUNGSTATE WITH A MIXED-LAYER, PYROCHLORE – HEXAGONAL TUNGSTEN BRONZE STRUCTURE, FROM VICTORIA, AUSTRALIA

WILLIAM D. BIRCH§

Geosciences Section, Museum Victoria, GPO Box 666, Melbourne, Victoria, 3001, Australia

IAN E. GREY

CSIRO Minerals, Box 312, Clayton South, Victoria, 3169, Australia

STUART J. MILLS

School of Earth Sciences, The University of Melbourne, Victoria, 3010, Australia

CATHERINE BOUGEROL

CEA Grenoble, 17, rue des Martyrs, F–38054 Grenoble, France

ALLAN PRING

Mineralogy Department, South Australian Museum, North Terrace, Adelaide, South Australia, 5000, Australia

STEFAN ANSERMET

Geological Museum and X-ray Laboratory, Institute of Mineralogy, UNIL–BFSH2, CH–1015 Lausanne–Dorigny, Switzerland

ABSTRACT

Pittongite, $(Na,H_2O)_x[(W,Fe)(O,OH)_3]$, $x \approx 0.7$ (IMA 2005–034), is a new mineral species from a tungsten deposit at Pittong, near Ballarat, in Victoria, Australia. The name recalls the discovery site, in turn derived from an Australian aboriginal word for *father*. The mineral occurs as glistening, creamy yellow encrustations of very thin (0.3–0.5 μm) platy crystals on etched blades of ferberite up to 4 cm long, enclosed in massive white reef quartz. It has formed by alteration of ferberite in a supergene environment in the presence of oxidizing, acidic solutions containing Na. The ferberite occurs in several hydrothermal quartz reefs, along with small amounts of bismuth, gold, bismuthinite, and other secondary tungstates and molybdates such as koechlinite and elsmoreite. Pittongite is hexagonal, space group $P\bar{6}m2$, with a 7.286(1), c 50.49(1) Å, V 2321.2 Å^3, refined from synchrotron X-ray powder-diffraction data. The density of the mineral could not be measured, but D_{calc} is 5.715 g/cm^3. Pittongite has a cream streak, estimated Mohs hardness of 2–3, and is non-fluorescent. Owing to the nature of the crystals, only limited optical data could be obtained; pittongite has an average index of refraction of 2.085, and is uniaxial negative. The strongest seven lines in the X-ray powder-diffraction pattern [d_{obs} in Å(I)(hkl)] are: 3.153(100)(00$\underline{1}$6,201), 3.111(91)(202,203), 1.823(76)(220), 1.578(64)(22$\underline{1}$6), 3.306(62)(116,10$\underline{1}$3), 2.450(59)(20$\underline{1}$3) and 5.956(52)(102,103). The average result of seven spot electron-microprobe analyses gave (wt%) Na_2O 2.97, K_2O 0.06, CaO 0.39, Fe_2O_3 5.66, Al_2O_3 0.51 and WO_3 84.15; H_2O determined by CHN analyzer 4.73%, for a total of 98.47 wt%. The empirical formula (on the basis of W + Fe^{3+} + Al = 1) is: $(Na_{0.22}H_2O_{0.44}Ca_{0.02}K_{0.003})_{\Sigma 0.683}(W_{0.82}Fe^{3+}_{0.16}Al_{0.02})_{\Sigma 1.00}[O_{2.70}(OH)_{0.30}]_{\Sigma 3.00}$. The crystal structure of pittongite is closely related to that of pyrochlore and can be derived from it by periodic, unit-cell-scale twinning parallel to $(111)_{pcl}$. This gives a stacking along c of pyrochlore blocks of two different widths, 6 and 12 Å, separated by pairs of hexagonal tungsten bronze (HTB) layers. TEM studies showed that disorder in the stacking sequence is common. The tungsten, together with minor iron and aluminum, occupies the octahedral sites in both the HTB and pyrochlore blocks. The sodium atoms and H_2O molecules occupy the A-atom positions of the pyrochlore blocks. Pittongite has structural and chemical similarities to phyllotungstite, $CaFe^{3+}{}_3H(WO_4)_6 \bullet 10H_2O$.

Keywords: pittongite, new mineral species, intergrowth, pyrochlore, hexagonal tungsten bronze, phyllotungstite, Pittong, Victoria, Australia.

§ *E-mail address*: bbirch@museum.vic.gov.au

Sommaire

Nous décrivons la pittongite, $(Na,H_2O)_x[(W,Fe)(O,OH)_3]$, $x \approx 0.7$ (IMA 2005–034), nouvelle espèce minérale provenant d'un gisement de tungstène à Pittong, près de Ballarat, Victoria, en Australie. Le nom rappelle le site de la découverte, qui à son tour est dérivé du nom aborigène pour *père*. Le minéral se présente en encroûtements jaune crémeux brillants en plaquettes très minces (0.3–0.5 μm) posées sur des lames de ferberite atteignant une longueur de 4 cm, encaissé dans du quartz laiteux massif. La pittongite s'est formée par altération de la ferberite dans un milieu supergène en présence de solutions oxydantes acides contenant du sodium. On trouve la ferberite dans plusieurs bancs de quartz hydrothermal, avec de faibles quantités de bismuth, or, bismuthinite, et autres tungstates et molybdates secondaires, par exemple koechlinite et elsmoreite. La pittongite est hexagonale, groupe spatial $P\bar{6}m2$, avec a 7.286(1), c 50.49(1) Å, V 2321.2 Å^3, paramètres affinés à partir de données en diffraction X prélevées sur poudre avec rayonnement synchrotron. La densité du minéral n'a pas pu être mesurée, mais la densité calculée est égale à 5.715 g/cm^3. La pittongite possède une rayure crème et une dureté de Mohs de près de 2–3, et elle est non-fluorescente. Vue la nature des cristaux, seules certaines des propriétés optiques ont pu être précisées; la pittongite possède un indice de réfraction moyen de 2.085, et elle est uniaxe négative. Les sept raies les plus intenses du spectre de diffraction X, méthode des poudres [d_{obs} en Å(I)(hkl)] sont: 3.153(100)(00$\underline{16}$,201), 3.111(91)(202,203), 1.823(76)(220), 1.578(64)(22$\underline{16}$), 3.306(62)(116,10$\underline{13}$), 2.450(59)(20$\underline{13}$) et 5.956(52)(102,103). Sept analyses ponctuelles avec une microsonde électronique ont donné (%, en poids): Na_2O 2.97, K_2O 0.06, CaO 0.39, Fe_2O_3 5.66, Al_2O_3 0.51 et WO_3 84.15; H_2O a été déterminé avec un analyseur CHN 4.73%, pour un total de 98.47%. La formule empirique, calculée sur une base de W + Fe^{3+} + Al = 1), est: $(Na_{0.22}H_2O_{0.44}Ca_{0.02}K_{0.003})_{\Sigma 0.683}(W_{0.82}Fe^{3+}_{0.16}Al_{0.02})_{\Sigma 1.00}[O_{2.70}(OH)_{0.30}]_{\Sigma 3.00}$. La structure cristalline de la pittongite est étroitement liée à celle du pyrochlore, et peut en être dérivée par macles périodiques à l'échelle de la maille, parallèles à $(111)_{pcl}$. Ceci donne un empilement le long de c de blocs de pyrochlore de deux différentes largeurs, 6 et 12 Å, séparés par des paires de couches de bronze à tungstène hexagonal. Nos observations par microscopie électronique en transmission font preuve de désordre répandu dans la séquence d'empilement. Le tungstène, de même que de faibles quantités de fer et d'aluminium, occupent les sites octaédriques à la fois du bronze à tungstène hexagonal et des blocs de pyrochlore. Les atomes de sodium et les molécules de H_2O occupent les positions A des blocs de pyrochlore. La pittongite ressemble à la phyllotungstite, $CaFe^{3+}{}_3H(WO_4)_6 \bullet 10H_2O$, des points de vue structuraux et chimiques.

(Traduit par la Rédaction)

Mots-clés: pittongite, nouvelle espèce minérale, intercroissance, pyrochlore, bronze à tungstène hexagonal, phyllotungstite, Pittong, Victoria, Australie.

Introduction

Secondary minerals resulting from the alteration of scheelite and the ferberite–hübnerite series (generally referred to as the wolframite group) are uncommon and easily overlooked. Simple secondary W-bearing species such as anthoinite, tungstite, mpororoite, hydrotungstite, ferritungstite and phyllotungstite are mostly white to cream or greenish, fine-grained powdery masses, only rarely manifested as well-formed microcrystals (Sahama 1981, Ercit & Robinson 1994). In some cases, the chemical formulae and crystal structures of these minerals are not well-established (*e.g.*, anthoinite). These phases tend to occur within etched crystals of ferberite and may have resulted from low-temperature hydrothermal or supergene alteration. The presence of coexisting sulfides of Cu or Bi increases the likelihood of more complex secondary W-bearing species, with phases such as cuprotungstite and russellite developing.

Strongly oxidized W–Mo–Bi deposits offer considerable potential for the discovery of new species. Recent investigations of pegmatite-hosted Bi–Mo–W assemblages in the New England district of New South Wales have resulted in the discovery of a range of rare secondary minerals (Rankin *et al.* 2002, Sharpe & Williams 2004, McKinnon *et al.* 2004), including the new species elsmoreite, $WO_3 \bullet 0.5H_2O$ (Williams *et al.* 2005).

There are numerous small deposits of tungsten within the Victorian region of the Paleozoic Lachlan Fold Belt (Campbell 2003). These are hosted by quartz veins associated with Late Devonian granitic intrusions. Many of these deposits were worked intermittently during the 19th century, with renewed interest in some of the larger deposits during World War II, but they have not been investigated mineralogically. One such deposit, located six km west of Linton and 35 km west of Ballarat, has been visited over the past decade by members of the Mineralogical Society of Victoria for its potential for mineral specimens. During one collecting excursion in 2003, a sample containing platy crystals of an unknown yellow mineral was found by Mr Steve Taylor on the dumps near the old main shaft. Investigation revealed this to be a new hydrated sodium ferric tungstate, which has been named *pittongite*. The name is taken from the former village of Pittong (an indigenous Australian word meaning father), which is now represented only by a road junction close to the mine site. The mineral data and name (IMA 2005–034) have been approved by the IMA Commission on New Minerals, Nomenclature and Classification prior to publication. The type specimen is preserved in the collection of Museum Victoria, registered as M48268.

Occurrence and Geology

The tungsten deposit near Pittong (37°40'S, 143°29'E) was opened in the 1860s and worked on and off until about 1913, mainly for the fine gold found with the manganoan ferberite (Baragwanath 1917, Herman 1920). The deposit consists of a number of quartz reefs trending N20°E and outcropping on a low ridge of weathered Ordovician metasedimentary rocks. The Mount Bute granite pluton, of Devonian age, underlies the countryside to the south of the deposit. Manganoan ferberite crystals in the quartz are commonly associated with brown needles of dravite, indicating hydrothermal development of the reefs during granite emplacement. Pittongite occurs in a specimen of reef quartz, about 8 × 6 × 5 cm, found on the dumps around the old shaft on the westernmost reef, formerly known as Bass and Watson's.

Other minerals present in ore samples submitted to the Victorian Mining Department in 1869 included chalcopyrite, pyrite, bismuth, bismuthinite, molybdenite, gold and silver, together with secondary copper and bismuth carbonates. Recent collecting has yielded additional species, including koechlinite (Birch 2001), scheelite, covellite, pharmacosiderite, plumbogummite, natrojarosite, elsmoreite, bismutite and bismoclite, the last two as products of the alteration of bismuth and bismuthinite.

Appearance and Physical Properties

Pittongite occurs as glistening, creamy yellow encrustations of platy crystals on etched blades of ferberite up to 4 cm long, enclosed in massive white quartz (Fig. 1). The mineral has partly replaced the ferberite, as well as occupying etched cavities in the surrounding quartz. The crystals are very thin (about 0.3–0.5 μm) curved plates with ragged outlines intergrown in open aggregates up to about 0.2 mm across (Fig. 2), or forming compact masses. The streak is cream, and the estimated hardness is 2–3 on the Mohs scale. The luster is pearly on the open aggregates of crystals, but earthy for compact material. Individual crystals are transparent under very high magnification. The density could not be accurately measured, but exceeds 4.4 g/cm^3, as crystals sink in Clerici solution. The density calculated from lattice parameters and composition is 5.715 g/cm^3.

The small size and platy nature of pittongite crystals meant that only limited optical data could be obtained. The mineral is uniaxial negative, with indices of refraction averaging 2.085, measured perpendicular to the platy surface and determined using liquids with Na light at 26°C.

Chemical Composition and Crystallography

Seven analyses were obtained using a Cameca SX50 microprobe in WDS mode at 15 kV, with specimen current of 20 μA and beam diameter 5 μm, at the University of Melbourne. Hematite (Fe), albite (Na), synthetic $KTaO_3$ (K), wollastonite (Ca), corundum (Al) and tungsten metal (W) were used as standards, with the ZAF correction method. No other elements with atomic

TABLE 1. CHEMICAL COMPOSITION OF PITTONGITE

Constituent	Mean	Range	Probe standard
Na_2O wt%	2.97	2.89–3.03	albite
K_2O	0.06	0.03–0.10	synthetic KTa
CaO	0.39	0.37–0.41	wollastonite
Fe_2O_3	5.66	5.39–5.83	hematite
Al_2O_3	0.51	0.45–0.66	corundum
WO_3	84.15	83.78–84.59	tungsten metal
H_2O^*	4.73	4.68–4.77	
Total	98.47		

* Determined with a CHN analyzer (see text).

FIG. 1. Portion of the type specimen (M48268) showing aggregates of pittongite on ferberite in quartz. The main patch is 17 mm long.

weights greater than eight were detected. The H_2O content was determined in duplicate using a Carlo Erba 1106 automatic CHN analyzer at the micro-analytical unit in the Research School of Chemistry, Australian National University.

In the mean analytical data (Table 1), we assume trivalent Fe and hexavalent W. The very thin platy nature of the pittongite crystals, hence the openness of their aggregates, is possibly the cause of the slightly low analytical total. Nevertheless, the mineral is very stable under the electron beam. The empirical formula, calculated on the basis of $(W + Fe^{3+} + Al) = 1$, is: $(Na_{0.22}Ca_{0.02}K_{0.003}H_2O_{0.44})_{\Sigma 0.683}$ $(W_{0.82}Fe^{3+}_{0.16}Al_{0.02})_{\Sigma 1.00}$ $[O_{2.70}(OH)_{0.30}]_{\Sigma 3.00}$. The crystal-structure basis for this formula is discussed below. The simplified formula for pittongite is $(Na,H_2O)_x[(W,Fe)(O,OH)_3]$, with $x \approx 0.7$.

Synchrotron X-ray powder-diffraction data were recorded using a high-resolution powder diffractometer at the Photon Factory (KEK), Tsukuba, Japan. Partial diffraction-rings were collected on three concurrent image plates, located 573 mm from the axially spinning sample. Data were collected at a wavelength of 0.80 Å and calibrated using an Y_2O_3 standard. The angular range of the data is from 3° to 123° in steps of ~0.01° of 2θ.

The powder pattern was indexed with the aid of precession photographs and selected-area electron-diffraction (SAED) patterns on individual crystals. These showed that the mineral has a hexagonal symmetry, with the only extinction (or pseudo-extinction) condition being for (00*l*) reflections with $l \neq 2n$. Refinement of the synchrotron diffraction-data (Table 2) was carried out using the Rietveld program SR5 (Hill & Howard 1986), yielding unit-cell parameters (hexagonal cell) *a* 7.286(1), *c* 50.49(1) Å and *V* 2321.2 Å^3. From the unit-cell parameters, *c*:*a* is equal to 6.93. The observed and calculated Rietveld patterns are shown in Figure 3. It was necessary to include hexagonal WO_3 (Gerand *et al*. 1979) as a second (minor) phase in the Rietveld fitting. The *h*–WO_3 is an alteration phase on the surface of the pittongite crystals (Grey *et al*. 2006).

The single-crystal diffraction patterns for pittongite show diffuse streaking along *c**, and the reflections with high *l* values in the powder pattern are broadened with respect to (*hk*0) reflections, indicating disorder between planes normal to the *c* axis. The nature of the disorder was investigated using transmission electron microscopy (TEM), conducted using a JEOL 4000EX microscope operated at 400 kV at CEA, Grenoble, France. In order to obtain relevant images containing the *c* axis, it was necessary to orient the thin platelets on their edge. This was very difficult to accomplish in the TEM; when we did succeed, the images were not well resolved because of the relatively thick direction of projection. Nevertheless, structurally interpretable fringe-patterns were obtained in a number of [100] and [110] zone-axis images, which helped in developing the structural model and determining the nature of the disorder. The results of these studies have already been published (Grey *et al*. 2006). The main findings are summarized in the next section.

Crystal Structure and Unit-Cell Composition

The crystal-structure study of pittongite, and of the related mineral phyllotungstite (Grey *et al*. 2006), revealed that the structures of both minerals are closely related to the pyrochlore structure. They can be described as being derived from pyrochlore by periodic twinning at the unit-cell scale, the twin planes being parallel to $(111)_{prc}$. These features are illustrated in Figure 4, showing a polyhedral representation of the pittongite structure in projection along [110]. The twin planes are located at layers of oxygen atoms, and the mirror-twin operation produces pairs of layers of corner-connected octahedra with a hexagonal tungsten bronze (HTB) motif. Andersson & Hyde (1974) proposed the term *chemical twinning* to describe this type of periodic unit-cell-scale twinning of a parent structure. Chemical twinning has been used to describe various structures, including that of orthopinakiolite (Takéuchi *et al*. 1978), wonesite and other micas (Veblen 1983) and sartorite and related sulfosalts (Hyde *et al*. 1979).

The structure of pittongite can alternatively be described in terms of a stacking sequence of pyrochlore blocks and HTB layers, parallel to $(111)_{prc} \equiv (001)_{HTB}$. The basic repeat-unit of pyrochlore normal to $(111)_{prc}$ planes has a thickness of 6 Å, whereas the repeat distance for HTB layer structures such as *h*–WO_3 is 3.7 Å. Pittongite has pyrochlore blocks of two different widths, 6 Å and 12 Å, as shown in Figure 4. The stacking sequence of pyrochlore blocks and HTB layers in pittongite is 12–3.7–12–3.7–6–3.7–6–3.7, with a repeat along *c* of ~50.49 Å.

TABLE 2. X-RAY POWDER-DIFFRACTION DATA FOR PITTONGITE

I	I_{calc}	d_{obs}	d_{calc}	*hkl*	*I*	I_{calc}	d_{obs}	d_{calc}	*hkl*
32 *	21	6.3	6.31	1 0 0	59 *	38	2.45	2.449	2 0 13
	41		6.262	1 0 1	9	2	2.384	2.385	2 1 0
52	44	6.0	6.122	1 0 2	8	4	2.104	2.103	3 0 0
	51		5.908	1 0 3	17	4	2.043	2.035	3 0 6
4	8	5.34	5.352	1 0 5		6		2.033	2 0 19
22	33	5.03	5.049	0 0 10	42 *	5	1.945	1.946	1 2 15
8 *	5	3.64	3.643	1 1 0		8		1.942	0 0 26
6	4	3.41	3.427	1 1 5	76 *	51	1.823	1.822	2 2 0
62 *	14	3.31	3.343	1 1 6	13 *	1	1.748	1.75	1 3 0
	8		3.308	1 0 13		8		1.75	2 2 24
100 *	55	3.15	3.156	0 0 16	23	9	1.716	1.714	1 1 26
	14		3.149	2 0 1		11		1.713	2 2 10
91	29	3.11	3.131	2 0 2	64 *	42	1.578	1.578	2 2 16
	71		3.101	2 0 3	35 *	12	1.463	1.462	4 0 13
21	38	3.01	3.011	2 0 5	13	1	1.446	1.448	2 3 0
30	26	2.951	2.954	1 1 10	16	6	1.429	1.427	3 0 26
	14		2.953	2 0 6	28 *	11	1.330	1.329	2 2 26

* These intensities include a contribution from the *h*-WO_3 surface phase.

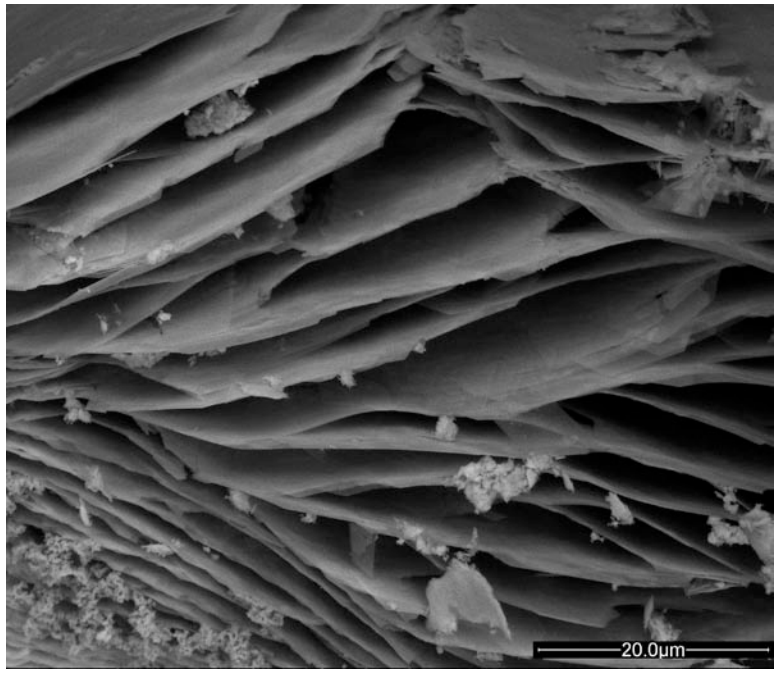

FIG. 2. Scanning-electron-microscope image of pittongite platelets.

The TEM images for pittongite reveal that the stacking sequence is not maintained over extended distances. Stacking faults due to local changes in the sequence of twin-plane separations commonly occur. This is illustrated in the [110] TEM image for pittongite shown in Figure 5. The bright spots in Figure 5 correspond to regions of low projected charge-density. A comparison with Figure 4 shows that these correspond to the hexagonal channels where the light atoms (Na, H_2O) are located. The separation between the (001) layers of hexagonal channels is 6 Å within the pyrochlore blocks and 9.7 Å (= 6 Å + 3.7 Å) across the twin planes. These two different cases are shown by the white lines in Figure 5, where an example of each type is labeled. The ordered structure for pittongite, as seen in Figure 4, corresponds to the sequence 9.7–9.7–9.7–6–9.7–6. An inspection of the TEM image in Figure 5 shows local changes to this sequence. The stacking disorder is most likely the result of non-equilibrium conditions during the low-temperature formation of pittongite. In contrast, Grey *et al.* (2007) have recently reported the formation of similar chemically twinned pyrochlore-type structures in the system Fe_2O_3–Bi_2O_3–Nb_2O_5 by high-temperature syntheses, and the resulting well-equilibrated phases show perfect long-range order in the pyrochlore–HTB stacking sequences.

In pittongite, the tungsten atoms, together with minor iron and aluminum, occupy the octahedral sites in both the HTB and pyrochlore blocks. The sodium atoms and H_2O molecules occupy the *A*-atom positions of the pyrochlore blocks (Grey *et al.* 2006). These are illustrated by the open circles in Figure 4. The unit-cell composition for pittongite can be calculated by combining the chemical data with the results from the structure analysis. The empirical formula for pittongite was calculated on the basis of $(W + Fe^{3+} + Al) = 1$ and is expressed in the form $A_xM(O,OH)_3$, by analogy with other tungstates, such as ferritungstite, in which the *A* site is partly vacant (Ercit & Robinson 1994). If all *A* sites available in pittongite were occupied, the general unit-cell formula would be $A_{28}M_{36}X_{108}$. By scaling the chemical data so that the number of atoms of $(W + Fe^{3+} + Al) = 36$ (*i.e.*, $Z = 36$), and with part of the analyzed H_2O assigned as OH for charge balance, the unit-cell composition for pittongite is: $(Na_{7.8}H_2O_{16.0}K_{0.1}Ca_{0.6})_{\Sigma 26.5}[W_{29.4}Fe_{5.8}Al_{0.8}]_{\Sigma 36}[O_{97.3}(OH)_{10.7}]_{\Sigma 108}$.

RELATIONSHIP TO PHYLLOTUNGSTITE

The similarity of the powder-diffraction patterns for pittongite and phyllotungstite, $CaFe^{3+}{}_3H(WO_4)_6{\bullet}10H_2O$ (Walenta 1984), suggests that they have related

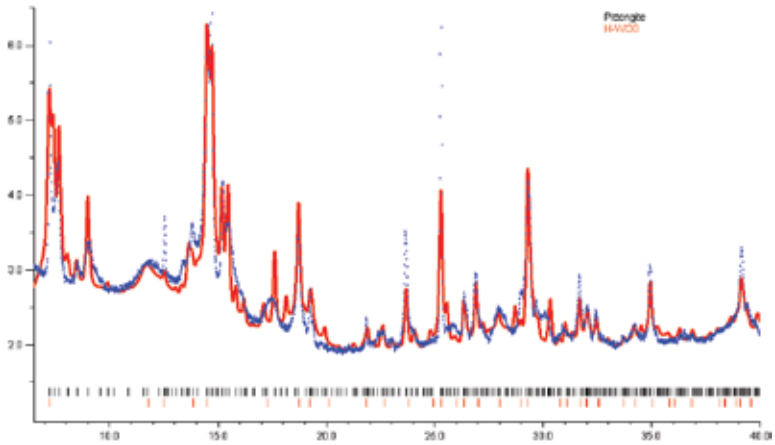

FIG. 3. Rietveld fit (solid line) to experimental synchrotron powder pattern (dotted line) for pittongite. Tick marks show the Bragg reflection positions for pittongite and for hexagonal WO_3, present as a minor surface-alteration phase.

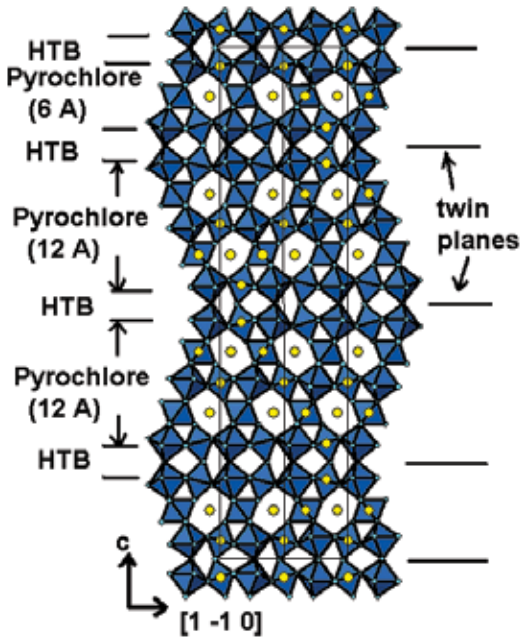

FIG. 4. The pittongite structure viewed in projection along [110], showing the $(W,Fe)_{36}(O,OH)_{108}$ framework as shaded octahedra. The Na and H_2O are shown by the open circles located in the hexagonal channels. The pyrochlore and HTB blocks are labeled, and the locations of the structural twin planes are shown.

structures. Phyllotungstite is reported to have an orthorhombic symmetry, with *a* 7.29 Å, *b* 12.59, Å, *c* 19.55 Å. However, Walenta (1984) commented that suitable single crystals were not available, and the cell parameters were determined from a powder pattern. The value of *b* is close to $\sqrt{3}a$, suggesting that the cell may be hexagonal. Using CELLREF (Laugier & Bochu 2000) to refine Walenta's powder data for both his orthorhombic cell and a hexagonal cell, an equally satisfactory fit to the published *d*-values was determined using the hexagonal cell with *a* 7.31(3) Å, *c* 19.55(1) Å. Compared to pittongite, the structure of phyllotungstite contains pyrochlore blocks of only one width and has the simple repeat sequence (3.7–6–3.7–6). The relationship between the structures of pittongite and phyllotungstite is discussed in more detail by Grey *et al.* (2006).

PARAGENESIS

Pittongite formed by the direct alteration of primary ferberite, presumably in a supergene environment in the presence of oxidizing, acidic solutions containing Na. The presence of elsmoreite in the deposit indicates that strongly acidic conditions (pH < 3) prevailed at times (Günter *et al.* 1989, Rankin *et al.* 2002). The timing of alteration is not known, and there are no other minerals on the type specimen of pittongite that could shed light on the paragenetic sequence.

Reis *et al.* (1992) reported that the low-temperature hydrothermal treatment of an acidified tungstate solution leads to phases with either a defect pyrochlore structure or a HTB structure. However, the mechanism by which ordered intergrowths of pyrochlore and HTB

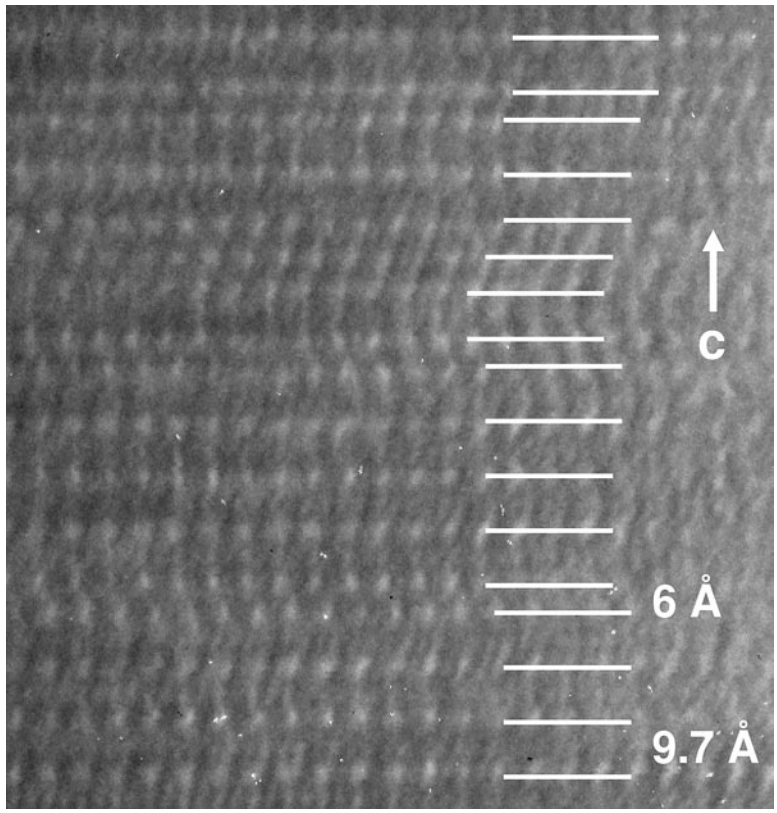

FIG. 5. TEM image of the [110] zone-axis from a thin crystal of pittongite.

structures develop during crystal growth requires a sophisticated explanation beyond our current understanding. The formation of pittongite is undoubtedly linked to the properties of W when hydrolyzed in acid solutions. The tetrahedral WO_4^{2-} ion dominates at near-neutral conditions, but as pH decreases, slow polymerization takes place (Baes & Mesmer 1976). A number of heteropolyanion species are formed depending on the acidity and dilution. Which of these were prominent close to saturation of the solution and precipitation is likely to have determined the basic crystal-structure framework of pittongite.

ACKNOWLEDGEMENTS

The collection of synchrotron data was undertaken at the Australian National Beam-line Facility at the Photon Factory, Tsukuba, Japan, with support from the Australian Synchrotron Research Program, which is funded by the Commonwealth of Australia under the Major National Research Facilities Program. Alexander Priymak assisted with the electron-microprobe analysis. Ben Healley, Museum Victoria, photographed the type specimen. The Associate Editor, Uwe Kolitsch, and two referees, provided helpful comments on the manuscript. SJM is supported by a Melbourne University postgraduate scholarship, CSIRO Minerals postgraduate scholarship and Museum Victoria 1854 scholarship.

REFERENCES

ANDERSSON, S. & HYDE, B.G. (1974): Twinning on the unit cell level as a structure-building operation in the solid state. *J. Solid State Chem.* **9**, 92-101.

BAES, C.F., JR. & MESMER, R.E. (1976): *The Hydrolysis of Cations*. John Wiley and Sons, New York, N.Y.

BARAGWANATH, W. (1917): Wolfram at Lintons. *Rec. Geol. Surv. Victoria* **4**(2), 19-20.

BIRCH, W.D. (2001): A note on koechlinite from Pittong, Victoria. *Aust. J. Mineral.* **7**(2), 77-79.

CAMPBELL, I.B. (2003): Other non-energy resources. *In* Geology of Victoria (W.D. Birch, ed.). *Geol. Soc. Aust., Spec. Publ.* **23**, 435-467.

ERCIT, T.S. & ROBINSON, G.W. (1994): A refinement of the structure of ferritungstite from Kalzas Mountain, Yukon, and observations on the tungsten pyrochlores. *Can. Mineral.* **32**, 567-574.

GERAND, B, NOWOGROCKI, G., GUENOT, J. & FIGLARZ, M. (1979): Structural study of a new hexagonal form of tungsten trioxide. *J. Solid State Chem.* **29**, 429-434.

GREY, I.E., BIRCH, W.D., BOUGEROL, C. & MILLS, S.J. (2006): Unit-cell intergrowth of pyrochlore and hexagonal tungsten bronze structures in secondary tungsten minerals. *J. Solid State Chem.* **179**, 3860-3869.

GREY, I.E., MUMME, W.G., VANDERAH, T.A., ROTH, R.S. & BOUGEROL, C. (2007): Chemical twinning of the pyrochlore structure in the system Bi_2O_3–Fe_2O_3–Nb_2O_5. *J. Solid State Chem.* **180**, 158-166.

GÜNTER, J.R., AMBERG, M. & SCHMALLE, H. (1989): Direct synthesis and single crystal structure determination of cubic pyrochlore-type tungsten trioxide hemihydrate, WO_3•$0.5H_2O$. *Mat. Res. Bull.* **24**, 289-292.

HERMAN, H. (1920): Bass and Watson's gold wolfram mine, Linton. *Rec. Geol. Surv. Vict.* **4**(2), 110-113.

HILL, R.J. & HOWARD, C.J. (1986): A computer program for Rietveld analysis of fixed wavelength X-ray and neutron powder diffraction patterns. *Australian Atomic Energy Commission, Rep.* **M112**.

HYDE, B.G., ANDERSSON, S., BAKKER, M., PLUG, C.M. & O'KEEFFE, M. (1979): The (twin) composition plane as an extended and structure-building entity in crystals. *Progress in Solid State Chem.* **12**, 273-327.

LAUGIER, J. & BOCHU, B. (2000): LMGP – program for the interpretation of X-ray experiments. INPG/Laboratoire des Matériaux et du Génie Physique, St Martin d'Hères, France.

MCKINNON, A.R., SHARPE, J.L. & WILLIAMS, P.A. (2004): Secondary minerals from the pegmatite-like Mo–Bi pipes of eastern New South Wales; a mineralogical cornucopia. *Twenty-seventh Annual Seminar of the Mineralogical Societies* (*Melbourne*), *Abstr.*, 23.

RANKIN, J., LAWRENCE, L.J., SHARPE, J.L. & WILLIAMS, P.A. (2002): Rare secondary bismuth, tungsten and molybdenum minerals from Elsmore, NSW. *Aust. J. Mineral.* **8**(2), 55-60.

REIS, K.P., RAMANAN, A. & WHITTINGHAM, M.S. (1992): Synthesis of novel compounds with pyrochlore and hexagonal tungsten bronze structures. *J. Solid State Chem.* **96**, 31-47.

SAHAMA, T.G. (1981): The secondary tungsten minerals, a review. *Mineral. Rec.* **12**, 81-87.

SHARPE, J.L. & WILLIAMS, P.A. (2004): Secondary bismuth and molybdenum minerals from Kingsgate, New England district of New South Wales. *Aust. J. Mineral.* **10**(1), 7-12.

TAKÉUCHI, Y., HAGA, N., KATO, T. & MIURA, Y. (1978): Orthopinakiolite, $Me_{2.95}O_2[BO_3]$: its crystal structure and relationship to pinakiolite, $Me_{2.90}O_2[BO_3]$. *Can. Mineral.* **16**, 475-485.

VEBLEN, D.R. (1983): Microstructures and mixed layering in intergrown wonesite, chlorite, talc, biotite and kaolinite. *Am. Mineral.* **68**, 566-580.

WALENTA, K. (1984): Phyllotunstit, ein neues sekundäres Wolframmineral aus der Grube Clara im mittleren Schwarzwald. *Neues Jahrb. Mineral, Monatsh.*, 529-535.

WILLIAMS, P.A., LEVERETT, P., SHARPE, J.L. & COLCHESTER, D.M. (2005): Elsmoreite, cubic WO_3•$0.5H_2O$, a new mineral species from Elsmore, New South Wales, Australia. *Can. Mineral.* **43**, 1061-1064.

Received July 25, 2006, revised manuscript accepted January 29, 2007.